A Case Study of Progressive Failure of Unsaturated Slope based on the Residual Shear Strength

Xiuhan Yang[1][0000-0001-5469-9863] and Sai K. Vanapalli[2][0000-0002-3273-6149]

[1] University of Ottawa, Ottawa, ON. K1N 6N5, Canada
[2] University of Ottawa, Ottawa, ON. K1N 6N5, Canada
sai.vanapalli@uottawa.ca

Abstract. The residual shear strength and strain-softening behavior play an important role in the stability analysis of slopes with fine-grained soils. This is because slopes constituting of both saturated and unsaturated soils typically undergo a large deformation prior to reaching failure condition. Several studies in the literature discuss about the influence of residual shear strength behavior in slope stability analysis of saturated soils. However, such studies are limited for unsaturated soils. In this paper, a case study results reported in the literature has been revisited to study the influence of the residual shear strength behavior on the slope stability of an unsaturated soil slope. A series of site investigations and shear strength test results are used to study the deformation and shear strength behavior of the slope. Slope stability analyses are performed using both peak and residual shear strength parameters based on the field and laboratory test results. This study highlights the importance of considering residual shear strength behavior in slope stability analysis of unsaturated fine-grained soils.

Keywords: Residual Shear Strength; Slope Stability Analysis; Unsaturated Soils

1 Introduction

The soil slopes that are in a state of unsaturated condition typically undergo a large deformation prior to reaching failure conditions [1, 2]. In these cases, the soil shear strength in the sliding zone will drop from the peak shear strength (PSS) to the residual shear strength (RSS) due to the large shear strain. The phenomenon is widely referred to in the literature as strain-softening behavior [3].

Many researchers have highlighted the role of RSS in the long-term slope stability analysis of saturated fine-grained soil slopes [4, 5]. These studies suggest that the distribution of shear strength is not uniform within a deforming slope. In the sliding zones that underwent large deformation, the shear strength of the soils reduces due to strain-softening behavior. The factor of safety (FOS) would be overrated if only PSS was used for slope stability analysis. This is because the RSS that governs the slope failure are typically lower than the PSS. More recently, the importance of RSS was highlighted in the slope stability analysis of unsaturated expansive soils [6]. Therefore, the strain-softening behavior based on RSS must be considered for the reliable

modelling, analysis and design of the unsaturated slopes that can undergo large shear deformation prior to reaching the failure condition.

The RSS behavior of saturated soils has been widely investigated in the literature [3, 7]. In recent years, the RSS behavior of unsaturated soils was investigated by a few researchers from experimental studies [8, 9, 10]. The experimental results have highlighted the significant influence of matric suction on the RSS and strain-softening behaviors of unsaturated soils. However, limited experimental data is presently available in the literature on the RSS of unsaturated soils. More importantly, studies related to simple yet reliable approaches for predicting the RSS of unsaturated soils are lacking.

A model for predicting the RSS of unsaturated soils [8] is summarized below:

$$\tau_r = c'_r + \left(\sigma_n - u_a\right) \tan \phi'_r + \left(u_a - u_w\right) (S^{\kappa_r}) \tan \phi'_r \qquad (1)$$

where $(\sigma_n - u_a)$ is the net normal stress; $(u_a - u_w)$ is the matric suction; c_r' and ϕ_r' are the RSS parameters of saturated soils; S is the degree of saturation; κ_r is the fitting parameter.

A reasonable performance has been validated based on the experimental results of suction-controlled ring shear tests conducted on unsaturated soils. However, S in this model should be estimated from an apparent soil-water characteristic curve (SWCC) obtained by using conventional pressure plate test from a specimen which has been sheared to the residual state. It will be time consuming to measure such a SWCC.

In order to simplify the required input parameters, a new model was developed to predict the RSS of unsaturated soils [11], which is based on the conventional SWCC. In this model, the residual shear strength of unsaturated soils can be expressed as:

$$\tau_r = c'_r + \left(\sigma_n - u_a\right) \tan \phi'_r + \left(u_a - u_w\right) (\frac{\theta - \theta_i}{\theta_s - \theta_i})^{\kappa_r} \tan \phi'_r \qquad (2)$$

where θ_s is the saturated volumetric water content; θ_i is the volumetric water content corresponding to the inflection point (i.e. the peak point of the derived function curve of SWCC equation, as shown in Fig. 1); κ_r is the fitting parameter for RSS, which is suggested to be 0.4 for a glacial till (Indian Head till) from Saskatchewan, Canada.

This RSS prediction model requires only the information of a conventional SWCC which can be obtained relatively easily from the laboratory. However, this model can only be applied within a relatively low suction range (i.e. $0 < \Psi < \Psi_i$). Eq. 2 shows when θ is less than θ_i, the RSS due to matric suction is zero. In other words, the suction cannot contribute to the RSS of unsaturated soils when it exceeds Ψ_i. This is inconsistent with the experimental observations reported by [10] that suction can still contribute to the RSS of unsaturated soils even when suction values are as high as 300 MPa. Therefore, Eq. 2 can only be used when $0 < \Psi < \Psi_i$. However, this is typically the range in which suction values are associated with the changes in the liquid phase flow and is important in conventional geotechnical engineering practice.
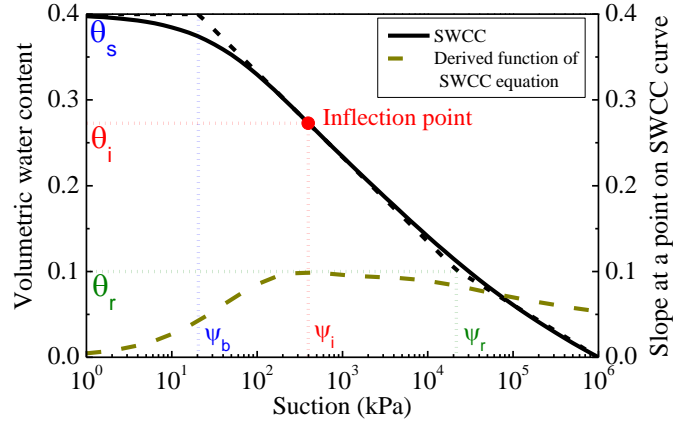
Fig. 1 The salient features of the soil-water characteristic curve (SWCC)

Geotechnical engineers understand the importance of RSS in the long-term stability analysis of both saturated and unsaturated slopes. However, there are limited case studies in the literature where the RSS concept was considered to interpret the behavior of unsaturated slopes in comparison to saturated soil slopes.

This paper introduces an old landslide which is reactivated recently due to the combined influence of rainfall infiltration and the Yangtze River water level variation at the slope toe. A series of direct shear test results were reported to study the RSS behavior of the saturated and unsaturated specimens. Based on the RSS parameters, a series of slope stability analyses were conducted using a commercial software, which is discussed in later sections. The results of the study are used to rationally interpret the landslide behavior at residual state conditions.

2   Site Investigation Studies

2.1   Study Area

The investigated Outang landslide is in Anping, Fengjie, China, which is about 177 km away from the Three Gorges Dam. The annual mean temperature and mean precipitation are 16.3 ℃ and 1147.9 mm, respectively. 70% of total annual precipitation occurs during summer season (i.e., from May to September).

The studied landslide is on the south bank of the Yangtze River, inclined from the South to the North. The Yangtze River flows in front of the slope toe, as shown in Fig. 2. The water level of the Yangtze River varies between 145 m and 175 m periodically every year.

2.2   Description of Landslide

The studied slope has a length of about 1800 m and a height of 600 m from the crest to the toe with an average gradient of 1:25. The average thickness of the sliding mass is about 50.8 m. The electron spin resonance (ESR) tests were used to determine the

age and sequence of landslides. The results indicated that the old landslide has occurred tens of thousands of years ago in three stages as shown in Fig. 2.
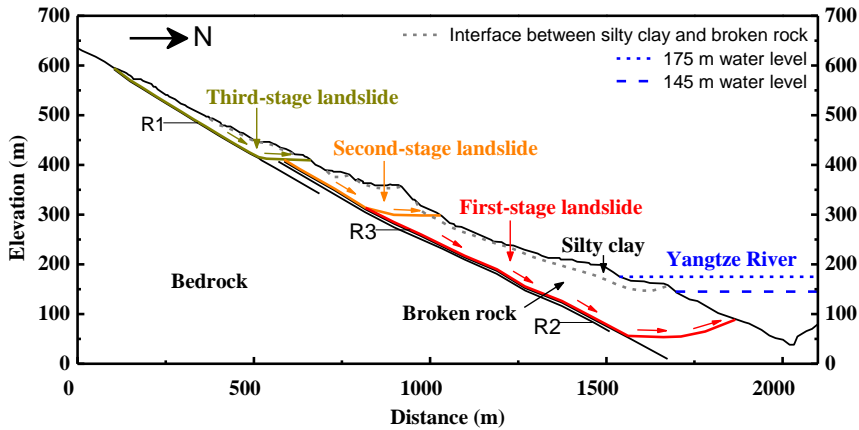
Fig. 2 Typical cross section of the Outang landslide (modified after [12])

Recently, Three Gorges Dam was constructed to the east of the Outang landslide and began to store water since 2003, which has significantly influenced the behavior of Outang landslide. The field observations indicated that the old landslide has started deforming again [12]. Firstly, large displacements of sliding mass and obvious sliding zones could be found at some monitoring points. A great number of cracks could be observed on the ground of the first-stage landslide. Similarly, settlements of roads and cracks on the ground could be observed in the third-stage landslide every year since 2003 especially during the rainy season. However, the second-stage landslide were still relatively stable. Thus, it can be concluded that the Outang landslide has been locally reactivated.

2.3 Rainfall and River water level data

Fig. 3 summarizes the rainfall data along with the variation of the Yangtze River water level from December 1st, 2010 to December 1st, 2014. Two typical variation curves of the ground surface displacement of the third-stage landslide from May 2012 to December 2014 are also presented in Fig. 3. This information is valuable for analyzing the relationship between the deformation behavior of the landslide and the variation of hydraulic/climatic condition, which is useful in the Outang landslide investigation.

From Fig. 3, it can be found the precipitation varied periodically during the measurement period (Dec 1st, 2010 – Dec 1st, 2014). Accordingly, the water level was also changed periodically based on the precipitation by the Three Gorges Reservoir. Every year the water level was decreased to a lowest value (145 m) during the rainy season to alleviate possible floods; then, it was increased to the highest value (175 m) during dry season.

The ground surface displacement increased for the measurement period, i.e., from May 2012 to December 2014. However, there is a significant increase in the ground surface displacement from May to September in 2012 and 2014, which is much greater than the period in 2013. In addition, the precipitation rate is significantly higher from May to September in 2012 and 2014 than that in the same period during 2013 under same condition of water level. These comparison studies suggest that the displacement variation was consistent with the variation in the precipitation rate. In addition, during the dry season (e.g., from January to May in 2013 and 2014), even though the precipitation is very low, there is still a slight increase in the ground surface displacement. This may be attributed to the decrease in the water level during this period. Therefore, it is reasonable to conclude that the displacement of the studied landslide can be attributed to the combined effect of the precipitation and water level variation.
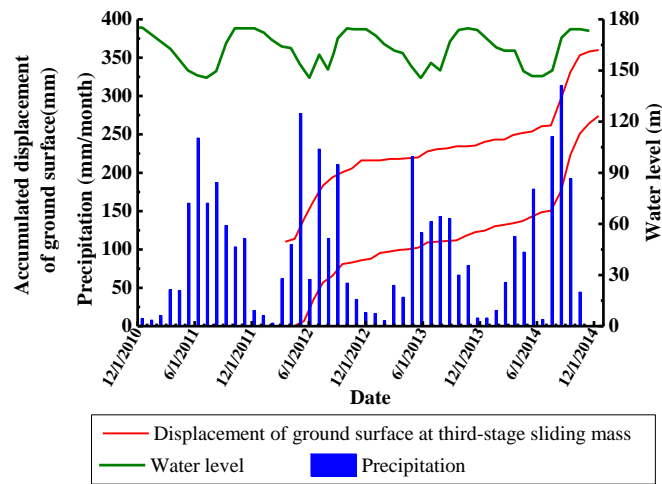
Fig. 3 Variation of the Yangtze River water level, precipitation and accumulated displacement of ground surface (modified after [12])

2.4   Material properties

The site investigation studies have shown that the sliding mass of the Outang landslide has two layers (Fig. 2): (i) a 3 – 20 m silty clay layer with gravels; (ii) a 10 – 85 m broken rock layer. Three weak zones (R1, R2 and R3) are sandwiched between the sliding mass and bedrock. The site investigation results show that the sliding mass moved along the R1 (10 – 35 cm claystone layer) and R3 (40 – 70 cm clay layer) weak zone.

Several undisturbed soil samples were collected from the silty clay layer, R1 and R3 weak zone. A series of laboratory tests were conducted to determine the physical and shear strength properties of the soils, which were reported in [12] and summarized in Table 1. A series of consolidated undrained direct shear tests were conducted on both the natural and saturated soil samples of R1 and R3. In addition, a series of

6

quick undrained direct shear tests were conducted on the natural and saturated soil samples of silty clay.

Table 1. Physical and mechanical properties of soils (summarized from [12])

	Plasticity index	Liquid index	Specific gravity	Natural specimen (Unsaturated)				Saturated specimen			
				c_p' (kPa)	ϕ_p' (°)	c_r' (kPa)	ϕ_r' (°)	c_p' (kPa)	ϕ_p' (°)	c_r' (kPa)	ϕ_r' (°)
silty clay	12.3	-0.02	-	45.9	14.6	27.0	11.3	34.7	12.4	21.6	9.2
R3	11.1	0.17	2.70	36.6	14.7	27.8	11.5	30.0	12.5	24.2	9.3
R1	10.7	0.15	2.71	52.4	18.0	29.0	12.9	37.8	12.1	24.7	9.5

3 Slope Stability Analyses

3.1 Schematic of slope used for numerical modelling

A series of numerical modelling studies were conducted based on the PSS and RSS parameters using the commercial software Geostudio [13]. Fig. 4 presents the numerical model of the landslide. In this numerical model, several assumptions were made to simplify the analyses. Firstly, the surface of the slope was simplified by neglecting some minor changes in the gradient of the real slope surface. Secondly, only R1 and R3 weak zone were considered in the numerical model. The R2 weak zone was neglected in the numerical model, because the slip surface did not go through it. The thickness of the R1 and R3 were both assumed equal to 0.5 m. Lastly, the three landslides that have occurred in a sequence were considered to occur at the same time. In other words, one slip surface was used in the numerical model to replace the slip surfaces in three stages.
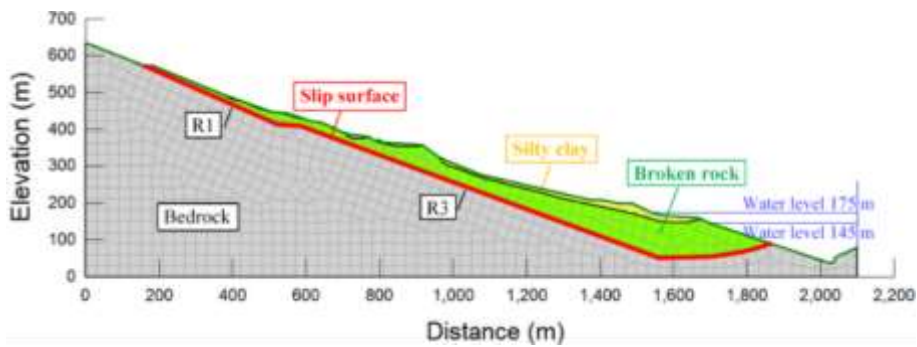
Fig. 4 Schematic of the slope used in the numerical modelling

3.2 Calculation procedures

In this numerical model, the combined influence of rainfall infiltration and variation of the water level were simulated. The variation of the FOS of the slope with time under the combined influence of these two factors was studied. For this purpose, three steps were involved in the numerical analysis. They can be described as:

(1) Steady-state seepage analysis: The boundary conditions on the left boundary and the slope surface below the water level (elevation = 175 m) were set as the constant total head boundary condition. Then, a steady-state seepage analysis can be conducted using Seep/W to simulate the pore water pressures in the slope under no precipitation and variation of the water level.

(2) Transient seepage analysis: Based on the numerical model in Step (1), a specific boundary condition was applied on the slope surface to model the precipitation and variation of the water level. Then, a transient seepage analysis was conducted to calculate the pore water pressures in the slope at different times.

(3) Slope stability analysis: Based on the numerical model in Step (2), the values of FOS of the slope at different times can be calculated using the Slope/W and RSS (or PSS) parameters.

3.3 Boundary conditions

The unit flux on the bottom and right boundary was set as 0 m/s; i.e. no flow occurred on those two boundaries. The total head on the left boundary was constant at 525 m as suggested by [12].

In the steady-state seepage analysis, the total head on the slope surface below the elevation of 175 m (i.e., the highest water level) was set as 175 m.
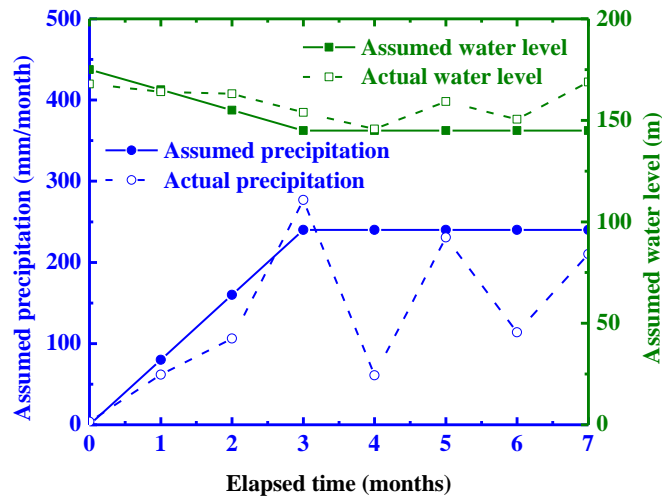
Fig. 5 Variation of actual and assumed values of precipitation and Yangtze River water level used in the numerical model (Feb 2012 – Sep 2012)

In the transient seepage analysis, the actual hydraulic/climatic condition was simulated by using the boundary conditions on the slope surface. From Fig. 3, it can be found that both the precipitation and water level varied periodically with time. Thus, only a representative period of one year (Feb 2012 – Feb 2013) was selected for the study. Additionally, during the wet season of this year, the shear strength decreased due to the rainfall infiltration and the seepage force increased due to the decrease in the water level. The composite influence of water level variation and precipitation can accelerate the slope failure. This means the wet season should be considered as the vulnerable period. Therefore, only the hydraulic/climatic condition for seven months (i.e., Feb 2012 – Sep 2012) was studied in this research. Fig. 5 presented the actual and assumed values of precipitation and water level variation. The unit flux on the slope surface above the elevation of 175 m was defined as a function of the elapsed time (continuous solid line with solid circles in Fig. 5). In addition, the total head on the slope surface below the elevation of 175 m was also defined as a function of the elapsed time (continuous solid line with solid squares in Fig. 5).

3.4   Material properties

In this numerical model, five types of materials are used, including silty clay, R1, R3, broken rock and bedrock (Fig. 4). Mohr-Coulomb model was used for all those materials. The hydraulic and shear strength parameters of those materials are described below.

The PSS and RSS parameters shown in Table 1 were used for the silty clay, R1 and R3. The effective shear strength parameters were not available in [12] for these materials. The parameters of R1 and R3 were derived from consolidated undrained direct shear test results and the parameters of silty clay were derived from quick undrained direct shear test results. By using this approach, the magnitudes of FOS will be underestimated. However, the research focus in this paper is directed on the slope stability considering the RSS behaviors. Although effective shear strength parameters were not used, the trends in variation of FOS of the simulated slope with time will be similar with that calculated using effective shear strength parameters. In other words, the slope behavior can still be analyzed considering the RSS.

In addition, the experimental results for the shear strength parameters of the broken rock and bedrock and the hydraulic properties of all those five materials were also not provided by [12]. However, a series of shear strength parameters and hydraulic properties have been suggested for all the five materials in the numerical models reported by [12], which were summarized in Table 2, Table 3 and Fig. 6. The SWCC parameters in Table 3 were obtained by fitting the SWCC suggested in [12] using the Fredlund & Xing equation [14]. These properties were also used in this study.

Table 2. Shear strength parameters in numerical model (summarized from [12])

	c_p' (kPa)	ϕ_p' (°)	c_r' (kPa)	ϕ_r' (°)
Broken rock	70	16.2	70	16.5
Bedrock	700	42	700	42

Table 3. Parameters of SWCC (summarized from [12])

	a	n	m	θ_s	θ_r	Ψ_i (kPa)
Silty clay	10.65	1.40	0.81	0.32	0.059	20
Broken rock	9.12	1.73	0.76	0.27	0.051	16
R1 and R3	9.07	1.53	0.59	0.30	0.094	20
Bedrock	9.81	1.46	0.70	0.05	0.012	20
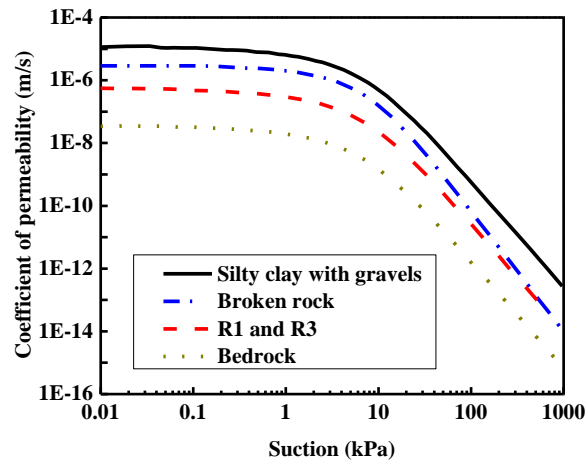
Fig. 6 Coefficient of permeability functions for different materials (modified after [12])

The RSS parameters of the broken rock and bedrock were assumed equal to the PSS parameters (shown in Table 2). That is because the slip surface only passed through the R1 and R3 weak zone; for this reason, the shear strength parameters of the broken rock and bedrock did not influence the FOS of the slope. Therefore, the assumption will not influence the FOS. In addition, the same SWCC and permeability function were used for the R1 and R3 weak zone, since they are both clays.

The prediction model for PSS of unsaturated soils was proposed by [15] as Eq. 3. The prediction models for RSS of unsaturated soils (e.g. Eq. 1 and Eq. 2) were described in the earlier sections of the paper. However, the apparent SWCC of the sheared specimens were not available in [12]. Therefore, the Eq. 1 cannot be used. In addition, the seepage analysis in this research showed the suction in the studied slope can reach as high as 800 kPa, which is much greater than Ψ_i of these soils. Therefore, Eq. 2 also cannot be used. For this reason, a model was postulated in this research to calculate the RSS in analogy with Eq. 3, which is expressed as Eq. 4.

$$\tau = c' + \left(\sigma_n - u_a\right)\tan\phi' + \left(u_a - u_w\right)(\frac{\theta - \theta_r}{\theta_s - \theta_r})\tan\phi' \tag{3}$$

$$\tau_r = c'_r + \left(\sigma_n - u_a\right)\tan\phi'_r + \left(u_a - u_w\right)\left(\frac{\theta-\theta_r}{\theta_s-\theta_r}\right)\tan\phi'_r \qquad (4)$$

where θ_r is the residual volumetric water content.

Eq. 4 was used to approximate the RSS of unsaturated soils in this research, since there is no RSS prediction model. The parameter, $(\theta-\theta_r)/(\theta_s-\theta_r)$ is typically used to describe the reduction in suction contribution at peak state with increasing suction. However, after peak state, some water menisci are destroyed, which contributes to a greater reduction in suction contribution at residual state than at peak state. In Eq. 4, $(\theta-\theta_r)/(\theta_s-\theta_r)$ was still used to describe the reduction in suction contribution. It tends to underestimate the reduction in suction contribution at residual state; i.e., Eq. 4 tends to overrate the RSS.

Finally, based on the PSS and RSS, the FOS of the slope can be calculated by using Morgenstern-Price method. The slip surface as shown in Fig. 4 was specified manually and used in the slope stability analyses.

4   Analyses of Results
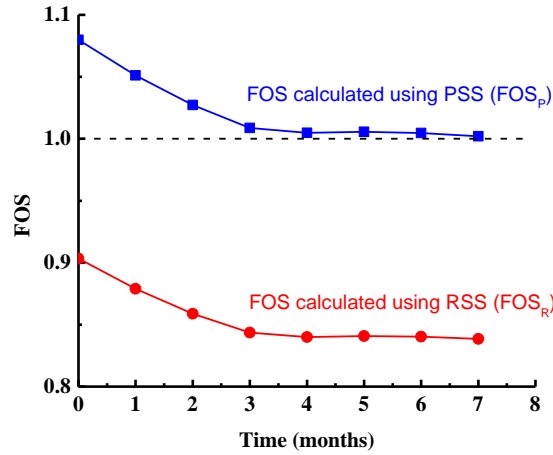
Fig. 7 Variation of FOS at peak and residual state with time under the combined influence of precipitation and water level variation

Fig. 7 presents the values of FOS at peak state (FOS$_P$) and FOS at residual state (FOS$_R$) under the combined influence of precipitation and water level variation. It can be found FOS$_P$ was always greater than 1.0 throughout the seven months period in spite of decreasing with time. In other words, the slope kept stable within the study period if the PSS was used to do analysis. These results however are not consistent with the field observations that a significantly large displacement has occurred (Fig. 3). This means the FOS was overrated due to the use of PSS. Therefore, the RSS should be considered for a reliable analysis of this landslide.

From Fig. 7, it can be found that FOS_R decreased almost linearly by about 6.6% within the first three months. Then, in the following four months, the decrease in FOS_R was much slower. From the third to seventh month, FOS_R decreased by 0.66%. In order to study the mechanisms associated with the landslide reactivation, soil suction profiles along the slip surface under the combined influence of the precipitation and water level variation are presented in Fig. 8. A sketch of the slope (shown in Fig. 4) is also presented in Fig. 8 to show the positions where the studied suctions were obtained. Two reasons can be found to interpret the reactivation of the landside.

The first reason is associated with the suction decrease caused by rainfall infiltration. The rainfall infiltration can cause an increase in the pore water pressure. Conversely, the decrease in water level can cause a decrease in the pore water pressure. From Fig. 8, it can be found the pore water pressures increased (i.e. the suction decreased) on the slip surface at the top of R1 and the connection between R1 and R3. This means the rainfall infiltration mainly influenced these two zones. Such a behavior may be attributed to the slip surface being shallow at the top of R1 (Fig. 8); thus, the infiltrated rainfall can reach the slip surface within a short time period. At the connection between R1 and R3, the bedrock is almost horizontal (Fig. 8); thus, the infiltrated rainfall tended to accumulate above the bedrock. Once the suction decreased on the slip surface, the RSS of the slide zone soils reduced as a result, which results in a decrease in FOS_R.

The second reason is the seepage force increase caused by decrease in the water level. From Fig. 8, it can be found that the pore water pressures decreased on the slip surface near the river, but they are still positive values. Therefore, the decrease in the water level did not influence the RSS of the slide zone soils. However, with decreasing water level, the difference between the water levels at the rear and front part of the slope increased. Consequently, the seepage force increased as a driving force in the sliding mass, which contributes to the decrease in FOS_R.
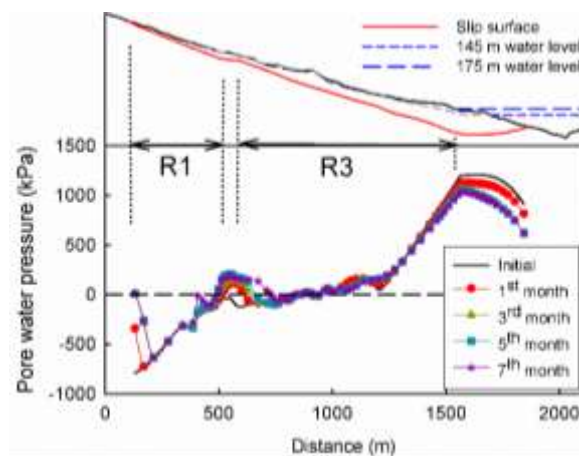
Fig. 8 Pore water pressure profiles along slip surface under the combined influence of precipitation and water level variation

12

In order to further study the influence of precipitation and water level decrease, two more numerical modelling studies were conducted based on RSS, which considered the influence of precipitation and water level decrease, separately. The variations of FOS_R with time in those two scenarios were presented in Fig. 9. In the first three months, the decrease in FOS_R caused by the water level decrease was much greater than that caused by the rainfall infiltration. This is because the slip surface which was influenced by the rainfall infiltration was far above the phreatic line. This means the matric suction on this part of slip surface was high and the volumetric water content was low. The contribution of the matric suction to RSS is much lower than that of the overburden pressure. Thus, the reduction in matric suction contribution can only cause a relatively small decrease in the RSS. In addition, the extent of the zones which were influenced by the rainfall infiltration was still limited. On most part of the slip surface, the RSS was not influenced by the rainfall infiltration. Therefore, the decrease in FOS_R caused by the rainfall infiltration was relatively small. In other words, it was the decrease in the water level that had a dominant contribution to the reduction in FOS_R within the first three months. From the third to seventh month, the continuous precipitation caused a further decrease in FOS_R. However, FOS_R increased slightly for the scenario where only the water level decrease was considered. This means, once the water level attains a relatively constant value, the rainfall infiltration should be the dominant factor that contributes to the reduction in FOS_R.
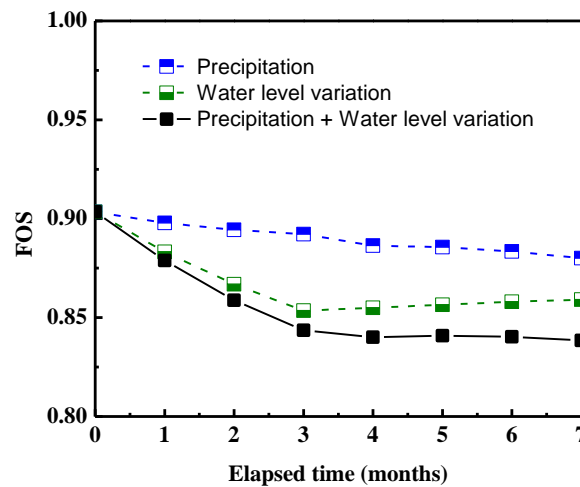
Fig. 9 Variation of FOS at residual state with time under different hydraulic/climatic conditions

In addition, it can also be found that the FOS_R was less than 1 initially when the precipitation and water level decrease did not start. This result is inconsistent with the field observations which indicated that the slope was stable before the precipitation and water level variation occurred. This can be attributed to an assumption in the numerical model that the RSS parameters were used throughout the slope, which did

not fit the actual case. In reality, the magnitude of shear strength should depend on the level of deformation. Initially, when no large deformation occurs, the shear strength of soils should be interpreted based on PSS parameters. After the precipitation increases and water level decreases, large deformations occur in some zones of the slope. As a result, in those zones with large deformations, the shear strength will be reduced to the RSS; however, the shear strength in other zones will be somewhere between the PSS and RSS depending on the magnitudes of deformation. Therefore, different values of shear strengths should be used in different zones of the slope according to the deformation level for reliably determining the FOS. If the RSS is used throughout the slope, the FOS will be underestimated. However, this approach provides a conservative value of FOS for the slope stability analysis.

5 Summary

In this paper, a reactivated landslide was revisited and analyzed. A series of site investigation and direct shear test results were reported to study the progressive failure behaviors of the landslide. The landslide was reactivated by the combined influence of the precipitation and water level variation. A series of numerical modeling were conducted using Geoslope to study the slope stability of the landslide based on the peak and residual shear strength. The key results are summarized below:

(1) The FOS will be overrated if PSS is used for slope stability analysis. Therefore, the RSS should be considered for a reliable modelling of the slope behavior.

(2) FOS_R decreased during the seven-month study period. This can be attributed to the reduction in the RSS of the slide zone soils caused by the rainfall infiltration and the increase in the seepage force caused by the water level decrease.

(3) During the period of the water level variation, the water level decrease should be the dominant factor that contributed to a significant reduction in FOS_R. Once the water level reached a relatively constant value, precipitation became the dominant factor contributing to the FOS_R reduction; however, the reduction rate was relatively smaller.

(4) In reality, different values of shear strengths should be used in different zones of the slope according to the deformation level. In other words, the RSS should be only used in the zones with large deformations; however, the values of shear strength between the PSS and RSS should be used in other zones depending on the magnitudes of deformation. If the RSS was used throughout the slope, the FOS would be underestimated. The slope stability analyses in this study are based on RSS; for this reason, they provide conservative results.

References

1. Widger, R.A. and Fredlund, D.G.: Stability of swelling clay embankments. Canadian Geotechnical Journal 16(1), 140-151 (1979).

14

2. Ng, C.W.W., Zhan, L.T., Bao, C.G., Fredlund, D.G. and Gong, B.W.: Performance of an unsaturated expansive soil slope subjected to artificial rainfall infiltration. Géotechnique 53(2), 143–157 (2003).
3. Skempton, A.W.: Long-term stability of clay slopes. Géotechnique 14(2), 77-102 (1964).
4. Potts, D.M., Kovacevic, N. and Vaughan, P.R.: Delayed collapse of cut slopes in stiff clay. Géotechnique 47(5), 953-982 (1997).
5. Locat, A., Jostad, H.P. and Leroueil, S.: Numerical modeling of progressive failure and its implications for spreads in sensitive clays. Canadian Geotechnical Journal 50(9), 961-978 (2013).
6. Qi, S. and Vanapalli, S.K.: Influence of swelling behavior on the stability of an infinite unsaturated expansive soil slope. Computers and Geotechnics 70, 154-169 (2016).
7. Lupini, J.F., Skinner, A.E. and Vaughan, P.R.: The drained residual strength of cohesive soils. Geotechnique 31(2), 181-213 (1981).
8. Infante Sedano, J.A. and Vanapalli, S.K.: Experimental investigation of the relationship between the critical state shear strength of unsaturated soils and the soil-water characteristic curve. International Journal of Geotechnical Engineering 5(1), 1-8 (2011).
9. Hoyos, L.R., Velosa, C.L. and Puppala, A.J.: Residual shear strength of unsaturated soils via suction-controlled ring shear testing. Engineering Geology 172, 1-11 (2014).
10. Romero, E., Vaunat, J. and Merchán, V.: Suction effects on the residual shear strength of clays. Journal of Geo-Engineering Sciences 2(1-2), 17-37 (2014).
11. Yang, X. and Vanapalli S.K.: Slope stability analysis of a slope based on the peak and the residual shear strength of unsaturated soils. Proceedings of 7th International Conference on Unsaturated Soils (UNSAT 2018), Hong Kong, China (2018).
12. Dai, Z.W.: Study on the deformation and failure mechanism of Outang landslide in the Three Gorges Reservoir Region, China. Ph.D. thesis, Chang'an University, Xi'an, Shanxi, China (2016). (in Chinese)
13. GeoSlope International Ltd.: Stability modeling with SLOPE/W: an engineering methodology. GEO-SLOPE International Ltd. Calgary, Alberta, Canada (2012).
14. Fredlund, D.G. and Xing, A.: Equations for the soil-water characteristic curve. Canadian Geotechnical Journal 31, 521-532 (1994).
15. Vanapalli, S.K., Fredlund, D.G., Pufahl, D.E. and Clifton, A.W.: Model for the prediction of shear strength with respect to soil suction. Canadian Geotechnical Journal 33(3), 379-392 (1996).